MODIFICATIONS TO EXISTING GROUND-MOTION PREDICTION EQUATIONS IN LIGHT OF NEW DATA

Gail M. Atkinson and David M. Boore
For Bull. Seism. Soc. Am. (final version)
Dec. 2, 2010

ABSTRACT

We compare our recent ground-motion prediction equations (GMPEs) for western North America (WNA) (Boore and Atkinson, 2008) (BA08) and eastern North America (ENA) (Atkinson and Boore, 2006 (AB06); Atkinson, 2008 (A08)) to newly-available ground-motion data. Based on these comparisons, we suggest revisions to our GMPEs for both WNA and ENA. The revisions for WNA affect only those events with $\mathbf{M} \leq 5.75$, while those for ENA affect all magnitudes. These are simple modifications to the existing GMPEs that bring them into significantly better agreement with data. The wealth of new data clearly demonstrates that these modifications are warranted, and we therefore recommend the use of the updated equations for seismic hazard analyses and other applications. More detailed studies are underway by many investigators (including ourselves) to develop a new generation of ground-motion models in both WNA and ENA "from scratch", through a comprehensive re-evaluation of source, path, site and modeling issues. In time, those more complete models will replace those proposed in this study. However, as the new models will be several years in development, we recommend using the modified models proposed herein – labeled BA08' (for WNA), AB06' (for ENA) and A08' (for ENA; to replace A08) – as interim updates to our existing models. The proposed models are in demonstrable agreement with a rich database of ground motions for moderate-magnitude earthquakes in both WNA and ENA, and are constrained at larger magnitudes by the BA08 magnitude and distance scaling.

INTRODUCTION

The availability of new data motivates the re-evaluation of our recent ground-motion prediction equations (GMPEs). For western North America (WNA; data are from shallow crustal earthquakes in California), compiled ShakeMap data for small-to-

moderate earthquakes have shown that the PEER-NGA (Pacific Earthquake Engineering Research Center, Next Generation Attenuation) GMPEs, including the Boore and Atkinson (2008) (BA08) equations, over-predict ground motions for small-to-moderate events ($\mathbf{M}$<6) in both northern and southern California (Atkinson and Morrison, 2009; Chiou et al., 2010). For eastern North America (ENA; data are from shallow crustal earthquakes in the northeastern U.S. and southeastern Canada), recent moderate events have produced ground-motion amplitudes that exceed the Atkinson and Boore (2006) (AB06) equations, especially at higher frequencies, by a significant margin. Furthermore, comparisons between BA08 and AB06 suggest that the magnitude scaling in AB06 may be too steep; moderate events are under-predicted by AB06, but large events may be over-predicted.

Detailed ground-motion studies are underway to produce new GMPEs in both western and eastern regions (e.g. NGA-West2, NGA-East projects; see http://peer.berkeley.edu/ngawest2/index.html, http://peer.berkeley.edu/ngaeast/, respectively), which will eventually supplant our current GMPEs. However, these developments are large projects that will not be complete for several years. It is thus important to have interim equations that can be used in seismic hazard analysis and other applications to remedy the known deficiencies of the existing GMPEs. In this article, we compare our recent GMPEs to newly-available ground motion data. Based on these comparisons, we suggest revisions to our GMPEs for both WNA and ENA. These are simple modifications to the existing GMPEs that bring them into significantly better agreement with data. We recommend the use of the modified GMPEs proposed herein in place of the original versions.

MODIFICATIONS TO BA08 (WNA) FOR SMALL-TO-MODERATE EVENTS

Our most recent GMPEs for WNA are the Boore and Atkinson (2008) PEER-NGA equations (see Power et al., 2008, and references therein). These equations were developed by a regression analysis of the PEER-NGA dataset, which contains strong-motion data compiled from shallow crustal earthquakes in active tectonic regions worldwide. The PEER-NGA strong-motion data are relatively sparse for small-to-moderate events ($\mathbf{M}$<5.5), which resulted in GMPEs that were not well-constrained for

M<5.5, especially with respect to their attenuation characteristics. Recent comparisons of the PEER-NGA equations with large ShakeMap databases from California earthquakes (www.earthquake.usgs.gov/earthquakes/shakemap) have shown conclusively that the PEER-NGA equations, including the BA08 equations, over-predict ground motions for events of **M**<6, while being in agreement with data for larger events (Atkinson and Morrison, 2009; Chiou et al., 2010). These findings are in accord with a body of studies in recent years that have pointed to the general problem of potential bias in GMPEs. There tends to be bias for small-to-moderate magnitudes for the case where the database is dominated by large events (Bommer et al., 2007; Cotton et. al., 2008); similarly, there may be bias for large magnitudes for the case where the database is dominated by small-to-moderate magnitude events (Campbell, 2008). The over-prediction of the PEER-NGA equations (and other GMPEs based on strong-motion data) for small-to-moderate events confuses comparisons between GMPEs in different regions, and may be consequential for seismic hazard studies in low-hazard areas (e.g. Douglas, 2010). It also has important implications for the development of GMPEs by methods which rely on GMPEs from more active regions as a reference level (e.g. Campbell, 2003, 2008; Atkinson, 2008). In this section, we compare the BA08 equations to both the PEER-NGA and California ShakeMap data, and suggest modifications that will bring them into reasonable agreement with data over a larger magnitude range (from **M**4 to 8). Chiou et al. (2010) have already suggested modifications to their PEER-NGA equations (Chiou and Youngs, 2008) in light of the ShakeMap data. We note that the functional form for the modifications to BA08 that we propose is such that there is no change in the predictions for events of **M**≥5.75.

Figure 1 plots the magnitude-distance distribution of the response spectra database used to evaluate the BA08 equations. The database is a merging of the PEER-NGA database (Chiou et al., 2008) for California events, as used by Boore and Atkinson (2008) and the ShakeMap database for small-to-moderate magnitudes in California compiled by Chiou et al. (2010); we refer to these databases as the NGA (Next Generation Attenuation) database and the SMM (small-to-moderate magnitude) database, respectively. Table 1 lists the number of events in each magnitude range, for each database. The SMM database contains the geometric mean of the horizontal-component

response spectra (PSA, the 5% damped pseudo-acceleration) at 3 periods (0.3, 1 and 3 s), and peak ground acceleration (PGA) and velocity (PGV), so these ground-motion parameters form the basis for our comparisons. For each record in the SMM database, Chiou et al. (2010) compiled as many of the NGA meta-data parameters as was practical; the SMM database includes the predictive variables used in the BA08 equations, namely moment magnitude (M), distance to the surface projection of the rupture (R_{jb}), V_{s30} (shear-wave velocity over the top 30 m), and focal mechanism (where available). It should be noted that the SMM database is not subject to the same high level of quality control as was the NGA database, as small events are not generally accorded the same level of detail in analysis of either event parameters or data processing. To evaluate the BA08 equations, we calculate the ratio of the observed ground-motion amplitudes to the predicted values (by BA08), for the given magnitude, distance and site condition, for both the NGA and SMM databases. (Note that because the GMPEs are developed in terms of the log of the ground-motion intensity parameter, the log of the ratio of observed to predicted motions is the formal residual between the observations and the predictions.) The focal mechanism is unknown for many of the SMM events, as detailed studies are not generally made for small events; in such cases the BA08 predictions are made for an unknown mechanism. We assume that the geometric mean of the horizontal components as compiled in the SMM database is equivalent, on average, to the orientation-independent horizontal-component mean used in the NGA database (Boore, 2010).

It has been noted in previous studies (Atkinson and Morrison, 2009; Chiou et al., 2010) that northern and southern California show statistically-significant differences between each other in terms of ground-motion attenuation rates, with northern California having faster attenuation. There are also some apparent differences in magnitude scaling between the two regions at lower magnitudes, but these are not persistent or systematic, and disappear at larger magnitudes. It is possible that the apparent magnitude-scaling differences are at least partly the result of the paucity of data in northern California in some magnitude ranges. After an initial separate evaluation of the residuals for northern and southern California, we decided to combine them for the purpose of this analysis. This is a practical decision, as it enables a single set of GMPEs for all of California (and by implication for all of WNA), and is consistent with the generic use of the PEER-NGA

equations for use in active shallow crustal regimes worldwide. There are undoubtedly regional differences in ground motions in different active tectonic regions, particularly in their attenuation, but distinguishing these differences is not within the purpose or scope of this study. In this study, we seek only a "first-order" correction to BA08 to bring it into reasonable agreement with the SMM data.

The approach taken to defining the required adjustments to the BA08 equations follows the philosophy of the Referenced Empirical Approach (Atkinson, 2008), which is a typical "model-building" approach. We plot the residuals versus distance, in several magnitude ranges, and seek by inspection a functional form to model the trends. We emphasize that this is a subjective modeling exercise aimed at defining a schematic representation of the trends, not a regression exercise aimed at achieving a statistical fit. We focus on the distance range $R_{jb} \leq 100$ km in modeling the trends, as the ShakeMap data become less reliable at larger distances. The developed equation for the ratio (Observed/Predicted) can then be used as a multiplier on the BA08 GMPE to adjust its predictions.

Figure 2 plots the residuals (in the format of the ratio of Observed/Predicted, plotted on a log scale; note that this is equivalent to residuals in log units plotted on a linear scale) for the response spectra (5% damped pseudo-acceleration, PSA, mean horizontal component) versus Joyner-Boore distance (R_{jb}) for events of **M** 4.0 to 4.5 (**M**4.25 magnitude bin); all of the data in this magnitude range are from the SMM database. We also compute the mean residual in log units (i.e. log(Observed/Predicted)) in distance bins that are 0.3 log(10) units in width, along with its standard deviation. The northern and southern California data are combined to calculate the mean; this ensures that multiple events are included in every magnitude range (of 0.5 units), as indicated in Table 1. It can be seen in Figure 2 that the residuals at 0.3s and 3s follow approximately the same trends, which are modeled by the solid line. (Note: the reason that the solid line is not a particularly good fit to the trends is because we chose to make the model frequency-independent, as discussed in the following.) Plots of the other parameters (PSA at 1.0s, PGA, PGV) indicate that they too follow the same residual trends (we show only two periods here, for brevity). Figures 3 to 5 show the corresponding plots for **M** 4.75, 5.25 and 5.75. For two of the magnitude bins (4.75, 5.25), we have data for California from

both the SMM and NGA datasets; the mean trends in the ratios of observations to predictions from these two sets are relatively consistent. There is some tendency towards ratios that are closer to unity in the NGA data, but this may be attributable to selective inclusion in the NGA data of "significant" moderate events (akin to the triggering problem with older records; see Joyner and Boore, 1981). For the **M**5.75 bin, the data are entirely from the NGA dataset (California events only).

The overall pattern that emerges from examination of the residual trends is that the average ratio of observations to predictions appears to be greater than 1 for small-to-moderate events at very close distances; the under-prediction at close distances becomes insignificant as magnitude increases. The amplitude of the residual trends decays with distance, with the slope of the trend approaching zero as magnitude increases. For **M**>5.5, the ratios of observations to predictions are not significantly different from unity. By inspection, these trends can be modeled by the functional form:

$$\log F_{BA08} = a - b \log(R_{jb}+10) \tag{1}$$

where *a* controls the near-source level of the residual in log units, *b* controls the decay slope with distance, and the "+10" mimics the observed amplitude saturation at close distances. For each magnitude range, an initial estimate of the value of *a* and *b* was made by trial-and-error, in order to approximately match the mean residuals. Due to the limited number of periods available in the SMM data, and the lack of compelling evidence for systematic frequency-dependence of the residuals amongst the available ground-motion parameters, we have chosen a frequency-independent model to represent the residual trends. The initial estimates were done by inspection, for each magnitude bin, rather than by a formal fitting procedure, as we are seeking to approximate the trends with a single function (i.e. single set of *a, b,* not dependent on period) that will approximate the behavior for 0.3, 1, 3s PSA, as well as PGA and PGV, for both the SMM and NGA databases, and in both northern and southern California. This is necessarily a subjective exercise, in which the function is a compromise between alternative data, rather than a "fit" to any particular set. The values selected for the function coefficients are plotted as a function of magnitude on Figure 6. They show well-behaved linear trends with magnitude, which are fit (by least-squares) to obtain:

$$a = 3.888 - 0.674\ \mathbf{M} \qquad\qquad \text{(for } \mathbf{M}{\leq}5.75) \qquad\qquad (2a)$$

$$a = 0. \qquad\qquad\qquad\qquad\quad \text{(for } \mathbf{M}{>}5.75) \qquad\qquad (2b)$$

$$b = 2.933 - 0.510\ \mathbf{M} \qquad\qquad \text{(for } \mathbf{M}{\leq}5.75) \qquad\qquad (3a)$$

$$b = 0. \qquad\qquad\qquad\qquad\quad \text{(for } \mathbf{M}{>}5.75) \qquad\qquad (3b)$$

For $\mathbf{M}{>}5.75$, note that $a = b = 0$, indicating that no adjustment to the BA08 equations is required at higher magnitudes. Thus the adjusted BA08 equations (BA08'), which can be used to predict ground-motion amplitudes for California events of $\mathbf{M}{\geq}3.5$ (Y') are simply:

$$Y' = Y\ F_{BA08} \qquad\qquad\qquad\qquad\qquad\qquad\qquad (4)$$

where Y' is the adjusted ground motion parameter value (PSA at a specific period, or PGA or PGV), Y is the predicted amplitude according to BA08, and the multiplicative function F_{BA08} is specified (in log10 units) by the following equation, which has a truncated linear form (on a log scale) with saturation at close distances:

$$\log\ F_{BA08} = \max(0,\ 3.888{-}0.674\mathbf{M}) - \max(0,\ 2.933{-}0.510\mathbf{M})\ \log\ (R_{jb}{+}10)$$

$$(5)$$

Figure 7 provides an illustration of the PSA predicted by the original BA08 and the adjusted BA08' from Equations (4) and (5), for B/C site conditions (760 m/s shear-wave velocity in top 30 m), for $\mathbf{M}{=}4.0$, for 0.3s and 1.0s PSA. In this figure, the changes in predicted amplitudes from the original to the adjusted equations are highlighted. The data from northern (NC) and southern (SC) California, for $3.75{\leq}\mathbf{M}{<}4.25$, are shown for comparison; these data have been corrected to B/C site condition values, using the site-response factors of BA08 (see Boore and Atkinson, 2008 for details of this correction). The BA08' equations are in significantly better agreement with the data (especially the NC data), in comparison to the original BA08 equations.

We propose that the BA08' equations be used in place of the BA08 equations for median predictions, to improve their performance for $\mathbf{M}{<}5.75$ earthquakes. We do not propose any adjustments to the standard deviations given by BA08 at this time. The standard deviations given in BA08 are implicitly reflective of the variability seen in larger events ($\mathbf{M}{>}5.5$), because the bulk of the data are from large events. This is

7

appropriate for the applications of these GMPEs to seismic hazard analysis. Any modifications to consider the potential impact of data from moderate earthquakes on variability would require more detailed study, preferably on a database with better quality control than the ShakeMap SMM database. At present, it is known that the ShakeMap SMM data have greater variability than strong-motion data, but this greater variability is of suspect significance.

MODIFICATIONS TO AB06 (ENA) IN MAGNITUDE SCALING

There are insufficient strong-ground motion data in ENA in the magnitude-distance ranges of engineering interest to derive robust GMPEs directly by regression analysis, as in the BA08 equations. Therefore, our 2006 GMPEs for ENA (Atkinson and Boore, 2006; AB06) were based on stochastic finite-fault simulations, where the key input parameters for the simulations were calibrated to ENA data to the extent possible. The key model parameters were the attenuation function, as calibrated from small-to-moderate magnitude data in ENA (Atkinson, 2004), and the stress parameter, which was set to an average value of 140 bars; the value for the stress parameter was loosely based on a calibration to a set of events (Atkinson and Boore, 2006). Since the publication of AB06, the ENA ground-motion database has grown significantly for small-to-moderate magnitude events (Assatourians and Atkinson, 2010), with the occurrence of many dozens of new events, providing thousands more records. Most of these events have been small (**M**<4), but three well-recorded moderate events have been of particular significance: 2005 **M**4.7 Riviere-du-Loup (Quebec), 2007 **M**5.0 Mt. Carmel (Illinois), and **M**4.7 2010 Val-des-Bois (Quebec). (Note: the 2005 event occurred during the final stages of preparation of AB06; ground-motion data for the event were plotted in AB06, but the preliminary moment magnitude that was assigned, **M**=5.0, is higher than the final moment determined by waveform modeling studies; see Boore et al., 2010.) All three of the recent events have had short-period amplitudes larger than those predicted by AB06, at distances in the range from 20 to 200 km. Given that these three events constitute our best data samples for moderate-magnitude ENA ground motions, and that the **M**5.8 1988 Saguenay earthquake also featured stronger-than-predicted short-period amplitudes, we consider this strong evidence that the AB06 equations are indeed "too low" in their short-

period predictions for moderate events at moderate distances. However we acknowledge that the ENA ground-motion database is still relatively sparse; it is possible that the last three events might be a biased sample. This possibility is a source of uncertainty in our revised GMPEs.

We evaluate the AB06 equations by comparison to the current ENA ground-motion database; it is also instructive to compare them to the (adjusted) BA08' equations. Figure 8 makes such a comparison for events of **M**4.5 to 5.5, for 0.3s; the bulk of the data on this plot are in the magnitude range from 4.7 to 5.0. We plot the horizontal-component data (both components), plus vertical-component data converted to horizontal-component using the frequency-dependent factors given in Siddiqqi and Atkinson (2002) for rock sites. To be consistent with the reference site condition of B/C for BA08', we plot the AB06 equations for B/C conditions. Therefore, we correct the recorded ENA ground-motion amplitudes to B/C conditions. This involves amplifying the motions recorded on hard-rock sites by the crustal amplification factors used in AB06 to make predictions for B/C, relative to those used to make predictions for hard rock, and adjusting the amplifications for the differences in the high-frequency attenuation parameter kappa (as used in AB06). This procedure ensures that the corrections used in both the model and the data are consistent. The factors applied to convert hard-rock values to equivalent values for B/C, all based on the parameters provided in AB06, are shown in Table 2. We acknowledge that there is considerable uncertainty in these crude correction factors from hard rock to B/C, which maps into uncertainty in making comparisons between ENA data and the BA08' GMPEs. For soil sites, the amplification factors of BA08 were used to model the expected amplification from B/C to the appropriate site class; this amplification was divided out of the observed motions to provide the equivalent motions for B/C. Table 3 summarizes the applied factors to convert soil amplitudes to equivalent values on B/C. As noted by Atkinson and Assatourians (2010), these soil amplification factors may greatly under-estimate the actual amplifications for ENA sites, due to the prevalence of soils overlying very hard rock, which sets up resonance conditions. This should be kept in mind when evaluating comparisons of ground-motion amplitudes recorded on soil to predicted values. Finally, to facilitate comparisons of the AB06 and BA08' equations, we have plotted the AB06

equations for the distance metric R_{jb} in Figure 8. A very approximate conversion was made from fault distance (R_{cd}) to surface distance (R_{jb}) for plotting purposes, to mimic distance saturation effects that are caused by focal depth effects which limit the nearest approach of a site on the surface to the fault (and thus not all values of R_{cd} are realizable). The AB06' predictions in R_{cd} (closest-distance to fault) have been plotted at roughly equivalent values of R_{jb} , by assuming that the depth to the top of the rupture surface is given by $Z_{tor} = 21\text{-}2.5\ \mathbf{M.}$ This equation specifies that the top of the fault is at a depth of 11 km for $\mathbf{M}$4, decreasing to a depth of 1 km for $\mathbf{M}$8; the Z_{tor} values were defined to be consistent with typical ENA focal depths of in the range of 8 to 12 km and the fault dimensions specified by AB06 (assuming hypocenters in the center of faults, with dip in the range from 45 to 90). We make the approximation that $R_{cd} \approx \sqrt{(R_{jb}^2 + Z_{tor}^2)}$. From Figure 8, we note that the AB06 equations tend to under-predict the observed motions for $\mathbf{M}$4.5 to 5.5 events in the distance range from about 20 to 200 km, though the predictions appear reasonable at larger distances; the under-prediction is particularly noticeably near 25 km and 60 km. Furthermore, the BA08' predictions exceed those of AB06 for moderate magnitudes, for distances $R_{jb} < 100$ km. Interestingly, the attenuation rate of AB06 and BA08' is similar in this distance range, as noted by Atkinson and Morrison (2009). Logically, we would expect short-period motions in ENA to be greater than those in California, because ENA earthquakes have higher stress drops (e.g. Kanamori and Anderson, 1975; Somerville et al., 1987; Atkinson and Hanks, 1995). Thus we may infer from Figure 8 that a larger stress parameter should have been used by AB06, at least for $\mathbf{M}$~5. At larger magnitudes, it is important to note that the AB06 predictions exceed those of BA08' at all distances. We might also infer that the shape of the attenuation curve may need revision; the attenuation followed by the data appears to be steep initially, as in AB06, but the AB06 curve does not do a good job of tying the distant observations to the near-source motions, through the shape of the "transition zone" at intermediate distances (see also Atkinson and Assatourians, 2010).

The AB06 equations included a stress adjustment factor that allows users to specify the stress parameter value to be applied. The default value suggested by AB06 was 140 bars. The use of the stress adjustment factor in AB06 provides a convenient mechanism by which to adjust the equations to bring them into better agreement with recent data, and

to achieve some logical consistency between eastern and western GMPEs. It should be noted that this is an "interim fix" rather than an ideal solution. In the longer term, a re-evaluation of both source and path effects in light of new data, and new insights into modeling techniques, will lead to a new generation of GMPEs for ENA. We suggest that a magnitude-dependent stress parameter should be used in the AB06 predictions to change the magnitude scaling of motions, such that eastern motions scale with magnitude in approximately the same way as do western motions. We believe that such an assumption regarding scaling is justified on the basis of its simplicity, in the absence of evidence to the contrary.   Relative to AB06 with the constant default stress value of 140 bars, we want the adjusted (AB06') equations to predict larger short-period motions at moderate magnitudes to better match ENA data.   However, we do not want to simply increase the stress value at all magnitudes, as this would result in unreasonably large short-period motions for large magnitude events. As shown on Figure 9, with the constant stress value of 140 bars in AB06, the predicted scaling of short-period motions with magnitude is much steeper in ENA than in the west. We therefore propose to use a magnitude-dependent stress parameter ($\Delta\sigma$) that will provide a match to the moderate-magnitude amplitudes in the ENA data (i.e. increase predicted amplitudes at moderate magnitudes), and will mimic the overall magnitude-scaling in BA08' (ie. decrease predicted amplitudes at large magnitudes). We propose that the AB06' equations should be implemented using:

$$\log \Delta\sigma = 3.45 - 0.2\ \mathbf{M} \qquad\qquad \mathbf{M} \geq 5 \qquad\qquad (6)$$

where these stress values are used to modify the default AB06 equations as given in Equation 6 (and Table 7) of Atkinson and Boore (2006, 2007). This equation provides a stress drop that equals 140 bars at $\mathbf{M}$=6.5, but increases by a factor of two to 280 bars at $\mathbf{M}$=5, while decreasing by a factor of two to 70 bars at $\mathbf{M}$=8.   For $\mathbf{M}$<5, we recommend capping the stress drop at the value of 280 bars.   The net effect of the magnitude-dependent stress drop is to significantly increase high-frequency amplitudes at all distances for $\mathbf{M} \leq 6$, while decreasing them for $\mathbf{M} \geq 7$; changes in predictions are modest for $\mathbf{M}$ 6 to 7, and for low frequencies. It is important to note that the stress values that are being recommended in Equation (6) are specific to the finite-fault algorithm used to

perform the computations for AB06; for other formulations or algorithms, different stress drop parameters might apply (see Atkinson et al., 2009).

On Figure 10, we show how the proposed AB06' implementation compares with the BA08' equations, for B/C site conditions. The comparison shows that the AB06' equations have the relationship with BA08' that we would expect to see, based on general knowledge of ground-motion data and scaling. Specifically, the AB06' predictions exceed those of BA08' at short periods, over all magnitudes and distances, which is expected due to the higher stress drop in ENA. At long periods, the BA08' motions may in some cases exceed those for AB06' at <100 km, which is reasonable due to larger crustal amplifications in California at long periods. At regional distances (>200 km), the AB06' motions greatly exceed the BA08' motions for all magnitudes at all periods, due to slower ENA attenuation. The scaling of motions with magnitude is approximately the same for AB06' and BA08'. We also note that the requirement for a stress parameter that decreases with increasing magnitude, in the context of AB06', is consistent with the studies of Atkinson et al. (2009) and Boore (2009), who showed that, due to the finite-fault normalization scheme used in the AB06 simulation algorithm, a larger stress drop is needed at moderate magnitudes to match equivalent point-source simulations, compared to that needed at large magnitudes.

Figure 11 plots the ratio of observations to predictions for rock data, for the current ENA database as compiled by Assatourians and Atkinson (2010), with respect to the AB06' (M-dependent stress) predictions. Soil data are not included in the plot, due to the possible undue influence of resonance effects as noted earlier. It is observed that the AB06' equations are a reasonable representation of the ENA data, although there is still a tendency towards under-prediction of amplitudes at close distances. Average ratios of observations to predictions for the plotted data at R_{jb}<50 km are a factor of approximately 1.2 at low frequencies, increasing to 1.4 at high frequencies. This amplitude offset appears significant, but it would disappear (ie. the average ratio would go to unity) if the assigned moment magnitudes for all events were adjusted upwards by 0.1 to 0.2 units. Thus the relationship between catalogue magnitudes (largely Nuttli magnitude, MN) and moment magnitude is important. For example, many of the largest residuals on Figure 11, especially at distances <200 km, come from the 2010 **M**5.0 Val-des-Bois and the

1988 **M**5.8 Saguenay earthquakes.   (Note: the Saguenay earthquake is the only event of **M**>5.5 in the ENA Toolbox database; the Toolbox data for Saguenay includes the seismographic records, but not the strong-motion data, as these have not been re-processed). The moment magnitudes for these events are considered well-determined by waveform modeling (unlike those for many of the smaller events, which are estimated by empirical relationships between **M** and MN). Moment magnitudes of 5.0 and 5.8 should correspond to MN values of about 5.5 and 6.1, respectively, based on magnitude conversions for an "average" event (see Atkinson and Boore, 1995); however the actual MN values reported for these events were 5.8 and 6.5, respectively (Geological Survey of Canada), indicating that the moment magnitudes of these events are not very representative of the ground-motion amplitudes as recorded on regional seismographic stations. There is significant inter-event variability in the conversions between magnitude scales, due to variability in source characteristics (e.g. stress drop). For short-period motions, catalogue magnitudes such as MN will provide a better prediction of the ground-motion amplitudes than will **M**, as they are anchored to the correct period range. This highlights the importance of the choice of magnitude scale in assessing GMPEs – and also in seismic hazard analysis. To minimize uncertainty in prediction of short-period amplitudes in ENA, it would actually make more sense to base both the magnitude-recurrence relations and the GMPEs in the seismic hazard analysis on MN rather than **M** (or on some other high-frequency magnitude measure, as suggested by Atkinson and Hanks, 1995). This point may also be appreciated by considering that the magnitude representation of an event maps into inter-event variability, whereas the variability in attenuation maps into intra-event variability. In concept, the inter-event variability would be zero if we could choose the "correct" magnitude representation for each event.   For example, the 0.2s inter-event residual terms for the Saguenay, and Val-des-Bois earthquakes are 0.35 and 0.15log units, respectively, for the assigned moment magnitudes of 5.8, and 5.0, in the distance range R<500 km (i.e. this is the average log residual over all records to 500 km, for each event). If we assigned the moment magnitudes of 6.1, and 5.4, corresponding to the Nuttli magnitudes for these events of 6.5and 5.8 (respectively), then the average inter-event residuals would reduce to 0.20, and -0.03 log units, respectively. At regional distances (>100 km), it is observed on

Figure 11 that the AB06' equations are over-predicting amplitudes, especially at short periods. These trends argue for an improved attenuation model in the future, particularly in connecting steeply-decaying amplitudes near the source to amplitudes at regional distances. A re-evaluation of the role of magnitude scales and conversions in GMPE assessment and hazard evaluation is also suggested. In the interim, we recommend that in implementing AB06, a magnitude-dependent stress drop (according to the stress adjustment factor algorithm provided by AB06) as given by Equation (6) be used; we refer to this GMPE as AB06'. We have posted tables of the resulting equations on our websites (see Data and Resources section) for the convenience of users. As for BA08', we do not propose any adjustments to the recommended variability to be associated with the revised median predictions.

MODIFICATIONS TO A08 (ENA) IN LIGHT OF BA08'

A final GMPE to revisit is the Referenced Empirical model of Atkinson (2008). This is a semi-empirical GMPE which was based on examining the residuals for ENA hard-rock ground motions, adjusted to B/C site conditions, against the BA08 equations for WNA. The idea was to develop an adjustment factor (like Equations 5 and 6) that could be multiplied by the BA08 ground motion predictions, in order to represent ENA ground motions. An advantage of the method is that it makes use of ENA data for calibration purposes, while retaining essential ground-motion scaling features contained in better-constrained GMPEs from more data-rich regions. The implicit assumption is that the magnitude scaling in the two regions should be the same; in this case, a multiplicative factor, depending only on distance and period, can be defined to represent differences in source levels and attenuation. The multiplicative factor is defined based on calibration with the moderate-magnitude ENA data. This model should be re-examined in light of the adjustments to BA08 for small-to-moderate magnitudes, and the new ENA data.

We calculate ratios of observations to predictions for the ENA rock data (NEHRP A and B classes; V_{s30}>760 m/s) compiled by Assatourians and Atkinson (2010), and adjusted to B/C conditions (760 m/s) as described in the previous section, against the

modified BA08' GMPEs. This will allow us to derive a new function by which to multiply BA08', in order to obtain empirically-constrained GMPEs for ENA. Figure 12 plots the ENA ratios of observations to predictions with respect to BA08', for all events with 3.5≤**M**<6.0, at 0.2s and 2.0 s; the largest magnitude category (**M**5.5 to 6.0) contains only one event, the **M**5.8 1988 Saguenay earthquake. Both horizontal data, and vertical data converted to horizontal (by multiplying by the H/V ratio for rock sites of Siddiqqi and Atkinson, 2002) are plotted (as described in the previous section). Note that an interesting feature of this residual trend, as seen on Figure 12, is that the Saguenay earthquake is no longer an obvious "outlier", at least for periods ≥ 0.2 s (Saguenay amplitudes are still high for 0.1 s, as seen in Figure 11); thus the proposed new Referenced Empirical GMPEs are not inconsistent with the Saguenay earthquake data amplitudes for periods ≥0.2s. (Periods of 0.2s and 2s were selected for the example plots in Figure 12 in order to demonstrate this.) The residual trends seen on Figure 12 are apparently independent of magnitude over the range plotted, but show a clear increasing trend at distances >100 km, as expected given the slower attenuation of ENA motions at regional distances. At distances <70 km, the residual trends are nearly constant, which suggests that attenuation rates for ENA are generally similar to those for BA08' at R<70 km.

To quantify the observed trends, we first overlay mean residuals (in log units) for all rock data in the **M** range 4.0 to 6.0, in distance bins 0.3 units in width; the distance bins are defined such that the bin at 100 km contains all of the data within the transition zone (70 to 140 km) from direct-wave to Lg spreading (see Atkinson, 2004). The mean trends are well fit by the function (in log(10) units, shown by solid lines of Fig. 12):

$$\log F_{ENA} = c(T) + d(T) R_{jb} \tag{7}$$

where T is period. This simple functional form is convenient because it is well constrained and robust, being nearly flat in log R_{jb} at close distances. Table 4 provides the coefficients of the residual factor log F_{ENA} for PSA at periods of 0.05s to 5.0s, PGA and PGV; Figure 13 plots the coefficient values. For periods <0.05s, the value at 0.05s may be used; for periods >5.0s, the value at 5.0s may be used. For intermediate periods, the coefficients may be linearly interpolated against log (period). Note that the

coefficients approach zero (they are not statistically significant) at long periods; this is expected since the motions at the longest periods are constrained by the seismic moment.

We obtain the A08' Referenced Empirical GMPE for ENA by adjusting the original BA08 predictions for both the small-to-moderate magnitude correction (Equations 4, 5) and the ENA correction (Equation 7). Thus the A08' Referenced Empirical GMPE is given by:

$$Y'_{ENA} = Y \; F_{BA08} \; F_{ENA} \tag{8}$$

where Y'_{ENA} is the predicted ground motion parameter value for ENA (PSA at a specific period, or PGA or PGV), Y is the predicted amplitude according to BA08, and F_{BA08} and F_{ENA} are the multiplicative functions specified by Equations 5 and 7. We provide tables of the A08' Referenced Empirical GMPE on our websites for the convenience of readers.

The new A08' Referenced Empirical GMPEs for ENA are in good agreement with ENA ground-motion data for moderate-magnitude events, as shown in Figures 14 and 15. Moreover, they are constrained to follow the empirically-established magnitude-scaling behavior from more data-rich regions, as encapsulated in the BA08 PEER-NGA equations, and modified to fit data in the moderate-magnitude range that dominates the ENA database. We therefore believe that these may be the most reasonable estimates available for median ENA ground-motion predictions at this time for many applications. However, it should be acknowledged that they smooth through potentially-significant Moho bounce effects, which may be particularly important to hazard contribution from large earthquakes at regional distances. The main difference between the Referenced Empirical and the Modified AB06 equations (also shown on Figures 14, 15) is in the shape of the attenuation curve. The Referenced Empirical GMPE has a smoother attenuation shape, with less influence of the transition zone on the attenuation curve. There are also some apparent differences at close distances, but these are related largely to the conversion of the R_{cd} distance measure used in AB06' to an equivalent R_{jb} (as used in BA08'), for the purpose of plotting comparisons (as described in the previous section). Future more detailed analysis can examine the attenuation shape in more detail, and how it ties regional observations to the source; we hope that these issues will be addressed by

the ongoing NGA-East Project. In the interim, these two alternative GMPEs for ENA (AB06' and A08') provide some measure of epistemic uncertainty in the median amplitudes and attenuation of ground motions for ENA earthquakes, based on current data and current general GMPE models.

CONCLUSIONS

We have proposed simple modifications to our existing median GMPEs for both WNA (BA08) and ENA (AB06, A08) to bring them into significantly better agreement with a wealth of new ground-motion data for small-to-moderate earthquakes. More detailed studies are underway by many investigators (including ourselves) to develop a new generation of ground-motion models in both WNA and ENA, through a comprehensive re-evaluation of source, path, site and modeling issues. In time, these more complete models will replace those proposed in this study. However, as the new models will be several years in development, we recommend using the modified models proposed herein – labeled BA08' (for WNA), AB06' (for ENA) and A08' (for ENA) – as interim updates to our existing models. The revised models update the median equations, but we propose no revisions to the associated variability. We note that predictions under the new BA08' WNA model do not differ from the original BA08, for events of $\mathbf{M} \geq 5.75$ (but are different at smaller magnitudes). The new AB06' and A08' GMPEs for ENA differ from the previous models (AB06 and A08) at all magnitudes, as we have modified the magnitude-scaling to be more consistent with that observed in data-rich western regions. The proposed models are in demonstrable agreement with a rich database of ground motions for moderate-magnitude earthquakes in both WNA and ENA, and are constrained at larger magnitudes by the BA08 magnitude and distance scaling.

DATA AND RESOURCES

The California database for the study was compiled from the PEER-NGA database (www. peer.berkeley.edu/nga/flatfile.html) and the Chiou et al. (2010) ShakeMap database, provided by Brian Chiou. The ENA database for the study was compiled by Assatourians and Atkinson (2010), and is available at www.seismotoolbox.ca. All figures were made with COPLOT (www.cohort.com). For the convenience of users,

tables of the AB06', BA08' and A08' predictions are posted on our websites, at www.seismotoolbox.ca and www.daveboore.com.

REFERENCES

Assatourians, K., and G. Atkinson (2010). Database of processed time series and response spectra for Canada: An example application to study of the 2005 MN5.4 Riviere du Loup, Quebec earthquake. Seism. Res. L., **81**, in press.

Atkinson, G. (2004). Empirical attenuation of ground motion spectral amplitudes in southeastern Canada and the northeastern United States. Bull. Seism. Soc. Am., **94**, 1079-1095.

Atkinson, G. (2008). Alternative ground-motion prediction equations for eastern North America from a Referenced Empirical Approach: Implications for epistemic uncertainty. Bull. Seism. Soc. Am., **98**, 1304-1318.

Atkinson, G. and K. Assatourians (2010). Attenuation and source characteristics of the June 23, 2010 Val-des-Bois, Quebec, earthquake. Seism. Res. L., **81**, 849-860.

Atkinson, G., K. Assatourians, D. Boore, K. Campbell and D. Motazedian (2009). A guide to differences between stochastic point-source and stochastic finite-fault simulations. Bull. Seism. Soc. Am., **99**, 3192-3201.

Atkinson, G., and D. Boore (1995). New ground motion relations for eastern North America. Bull. Seism. Soc. Am., **85**, 17-30.

Atkinson, G. and D. Boore (2006). Ground motion prediction equations for earthquakes in eastern North America. Bull. Seism. Soc. Am., **96**, 2181-2205.

Atkinson, G. and D. Boore (2007). Erratum to "Ground motion prediction equations for earthquakes in eastern North America". Bull. Seism. Soc. Am., **97**, 1032.

Atkinson, G. and T. Hanks (1995). A high-frequency magnitude scale. Bull. Seism. Soc. Am., **85**, 825-833.

Atkinson, G. and M. Morrison (2009). Regional variability in ground motion amplitudes along the west coast of North America. Bull. Seism. Soc. Am., **99**, 2393-2409.

Boore, D. (2009). Comparing stochastic point-source and finite-source ground-motion simulations: SMSIM and EXSIM. Bull. Seismol. Soc. Am., **99**, 3202-3216.

Boore, D. (2010). Orientation-Independent, Nongeometric-Mean Measures of Seismic Intensity from Two Horizontal Components of Motion.Bull. Seism. Soc. Am. **100**, 1830-1835.

Boore, D. and G. Atkinson (2008). Ground-motion prediction equations for the average horizontal component of PGA, PGV, and 5%-damped SA at spectral periods between 0.01s and 10.0 s. Earthquake Spectra, **24**, 99-138.

Boore, D., K. Campbell and G. Atkinson (2010). Determination of stress parameters for eight well-recorded earthquakes in eastern North America. Bull. Seism. Soc. Am., **100**, 1632-1645.

Campbell, K. W. (2003) Prediction of strong ground motion using the hybrid empirical method and its use in the development of ground-motion (attenuation) relations in eastern North America, *Bull. Seismol. Soc. Am.* **93**, 1012–1033.

Campbell, K. W. (2008) Hybrid empirical ground motion model for PGA and 5% damped linear elastic response spectra from shallow crustal earthquakes in stable continental regions: example for eastern North America, In *Proc., 14th World Conference on Earthquake Engineering*, Beijing, Paper No. S03-001.

Chiou, B., Darragh, R., Gregor, N., and Silva, W., 2008. NGA project strong-motion database, *Earthquake Spectra,* 24, 23 - 44.

Chiou, B. S.-J., and Youngs, R. R., 2008a. An NGA model for the average horizontal component of peak ground motion and response spectra, *Earthquake Spectra* 24, 173-216.

Chiou, B., R. Youngs, N. Abrahamson and K. Addo (2010). Ground motion model for small-to-moderate shallow crustal earthquakes in California and its implications for regionalization of ground motion prediction models. Earthquake Spectra, in press.

Cotton, F., G. Pousse, F. Bonilla, and F. Scherbaum (2008) On the discrepancy of recent European strong-motion observations and predictions from empirical models: analysis of KiK-net accelerometric data point-sources stochastic simulations, *Bull. Seismol. Soc. Am.* **98**, 2244–2261.

Douglas, J. (2010). Investigating possible regional dependence in strong ground motions, in Earthquake Data in Engineering Seismology, Springer Ltd., in press.

Joyner, W. and D. Boore (1981). Peak horizontal acceleration and velocity from strong motion records including records from the 1979 Imperial Valley, California, earthquake. Bull. Seism. Soc. Am., **71**, 2011-2038.Kanamori, H. and D. Anderson (1975). Theoretical basis of some empirical relations in seismology. Bull. Seism. Soc. Am., **65**, 1073-1095.

Power, M., Chiou, B., Abrahamson, N, Y. Bozorgnia, T. Shantz and Roblee, C. (2008). An overview of the NGA project. Earthquake Spectra, **24**, 3-21.

Siddiqqi, J. and G. Atkinson (2002). Ground motion amplification at rock sites across Canada, as determined from the horizontal-to-vertical component ratio. Bull. Seism. Soc. Am., **92**, 877-884.

Somerville, P., J. McLaren, L. Lefevre, R. Burger and D. Helmberger (1987). Comparison of source scaling relations of eastern and western North American earthquakes. Bull. Seism. Soc. Am., **77**, 322-346.

Table 1 – Number of events included in residual analysis, from SMM and NGA
databases, in northern (NC) and southern (SC) California, for each magnitude range
(in 0.5 unit **M** intervals; 3.0≤**M**≤3.5, 3.5≤**M**<4.0, etc.).

M	SMM - NC	SMM - SC	NGA - NC	NGA - SC
3.25	3	35	0	0
3.75	30	56	0	0
4.25	17	28	0	0
4.75	3	7	1	3
5.25	2	7	4	2
5.75	0	0	4	5
6.25	1	0	5	1
6.75	0	0	1	5
7.25	0	0	1	3

Table 2 – Factors used to convert ENA hard-rock ground motions to equivalent
amplitudes for B/C site conditions. A-amp, BC-amp are crustal amplification factors
for hard rock, B/C sites, respectively. A-kappa, BC-kappa are multiplicative
adjustments for kappa for hard rock, B/C sites (all based on AB06; kappa=0.005 for
A, kappa=0.02 for B/C). Product of A-amp*A-kappa=A-tot (same for BC). Final
correction factor AtoBC=A-tot/BC-tot.

Period(s)	A-amp	BC-amp	A-kappa	BC-kappa	A-tot	BC-tot	AtoBC
0.02	1.41	2.50	0.46	0.04	0.64	0.11	0.17
0.10	1.41	2.36	0.85	0.53	1.20	1.25	1.04
0.20	1.36	2.25	0.93	0.73	1.26	1.65	1.31
0.32	1.29	2.10	0.95	0.82	1.23	1.73	1.41
0.50	1.22	1.88	0.97	0.88	1.18	1.66	1.40
1.00	1.13	1.51	0.98	0.94	1.11	1.42	1.27
2.00	1.00	1.29	0.99	0.97	0.99	1.25	1.26
3.20	1.00	1.20	0.99	0.98	0.99	1.18	1.18
5.00	1.00	1.11	1.00	0.99	1.00	1.10	1.10
10.00	1.00	1.00	1.00	0.99	1.00	0.99	1.00
PGA	1.41	2.50	0.85	0.53	1.20	1.25	1.04
PGV	1.22	1.88	0.96	0.86	1.17	1.61	1.37

Table 3 – Factors used to convert soil amplitudes to equivalent values for B/C site
conditions (based on BA08). A factor of 1.0 was assumed for B to B/C.

Period (s)	C to BC	D to BC	E to BC
0.02	0.89	0.77	0.65
0.05	0.89	0.77	0.65
0.10	0.89	0.77	0.65
0.20	0.88	0.75	0.61
0.32	0.83	0.66	0.49
0.50	0.78	0.57	0.38
1.00	0.75	0.52	0.32
1.96	0.74	0.51	0.31
3.13	0.74	0.50	0.30
5.00	0.73	0.50	0.30
10.00	0.76	0.55	0.35
PGA	0.90	0.77	0.65
PGV	0.78	0.57	0.38

Table 4 – Coefficients for ENA Referenced Empirical GMPEs (relative to BA08').
Factor $\log F_{ENA} = c + d\ R_{jb}$. Use linear interpolation of c, d versus log period for
other periods.

period(s)	c	d
≤0.05	0.417	0.00192
0.10	0.245	0.00273
0.20	0.042	0.00232
0.30	-0.078	0.00190
0.50	-0.180	0.00180
1.00	-0.248	0.00153
2.00	-0.214	0.00117
3.03	-0.084	0.00091
≥5.00	0.	0.
PGA	0.419	0.00211
PGV	0.450	0.00039
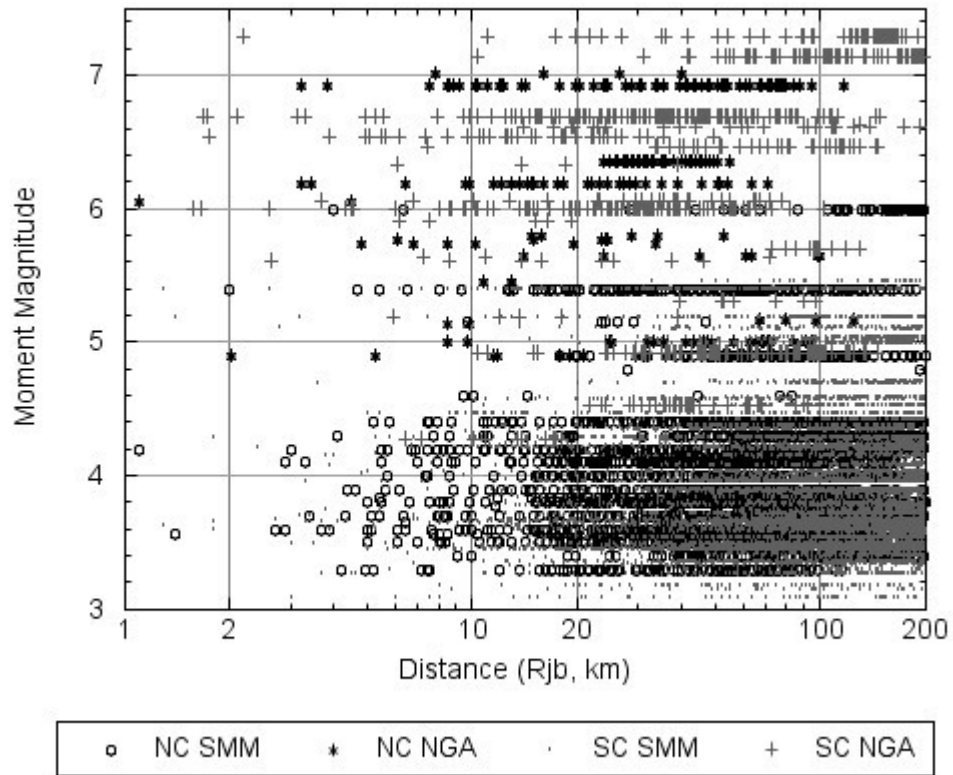
Figure 1 – Magnitude-distance distribution of data from Northern California (NC) and Southern California (SC) in the NGA and SMM (Chiou et al., 2010) ShakeMap databases.
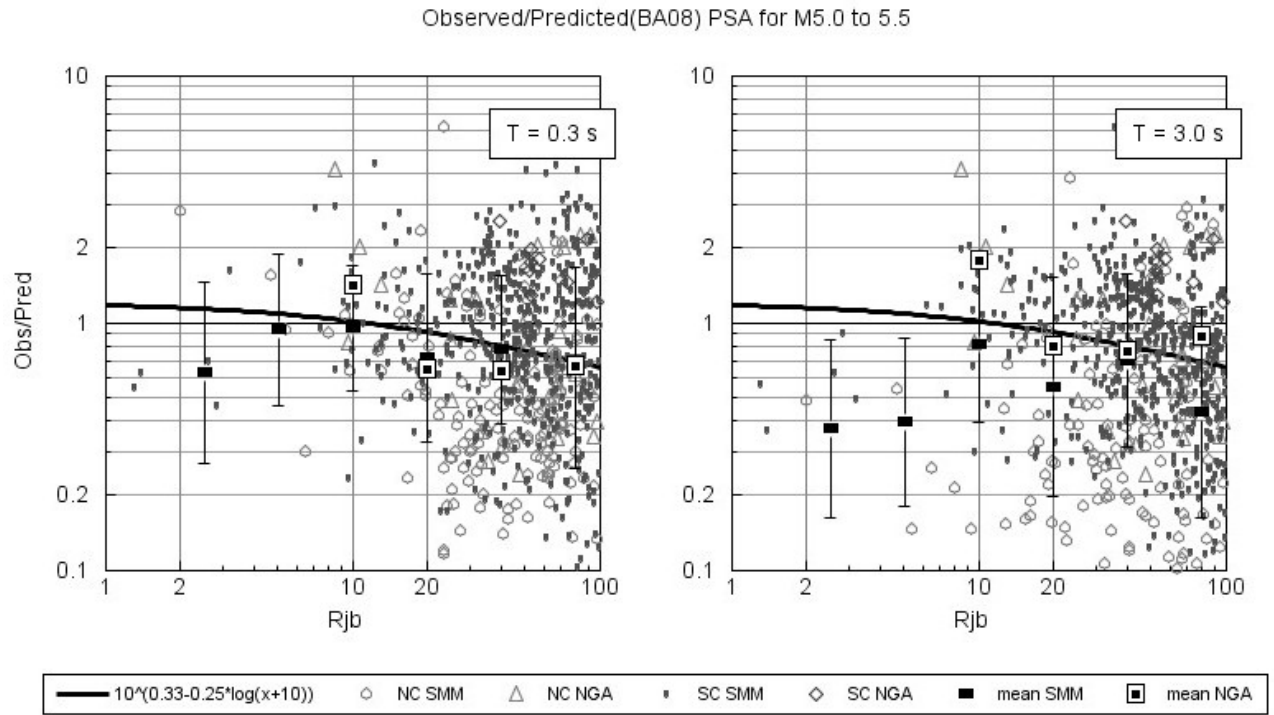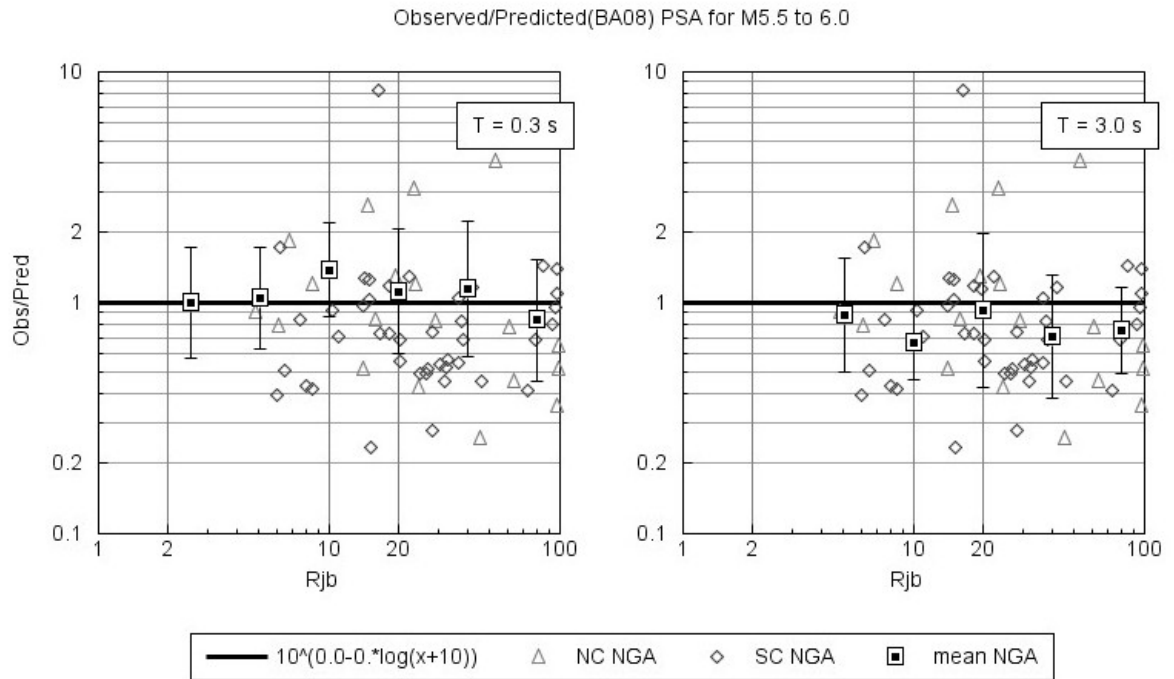
Observed/Predicted(BA08) PSA for M4.0 to 4.5
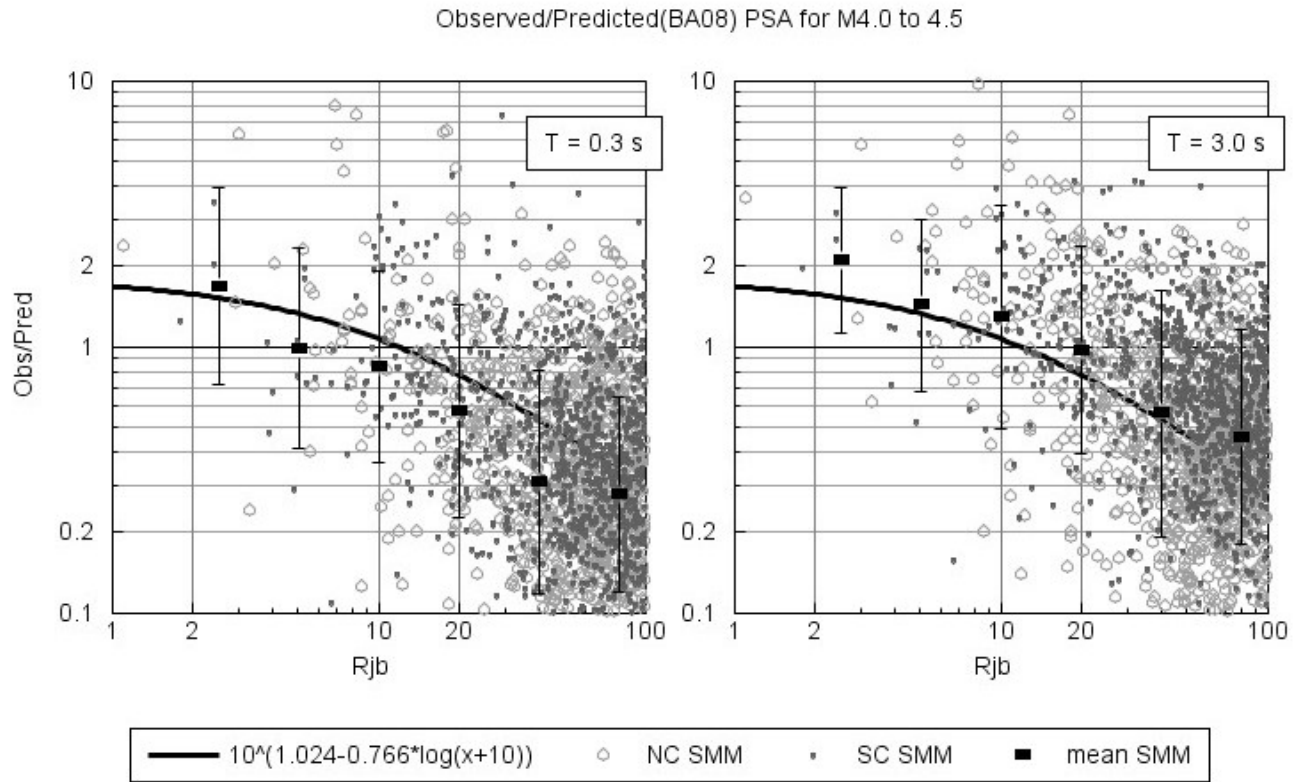
Figure 2 – Ratio of observed to predicted (by BA08) PSA for California earthquakes
(NC=northern, SC=southern) of 4.0≤**M**<4.5, at periods 0.3 and 3s. All data in this
magnitude range are from the SMM dataset. Heavy boxes show mean ratios (and
standard deviation) in distance bins (SMM), while heavy line shows function chosen
to represent the mean trend (**M**4.25).
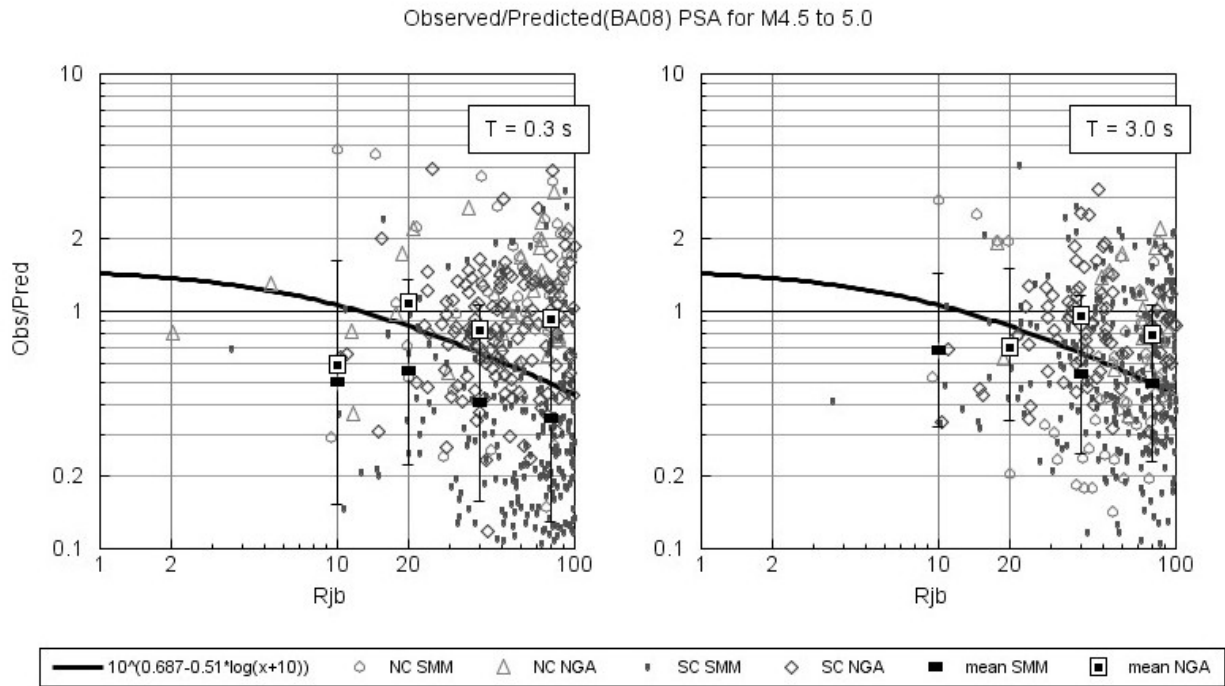
Figure 3 – Ratio of observed to predicted (by BA08) PSA for California earthquakes
(NC=northern, SC=southern) of 4.5≤**M**<5.0, at periods 0.3 and 3s. Data are shown
for both the SMM and NGA datasets. Heavy solid boxes show mean ratios (and
standard deviation) in distance bins for SMM; means are also shown for the NGA
dataset. Heavy line shows function chosen to represent the mean trend (**M**4.75).

Observed/Predicted(BA08) PSA for M5.0 to 5.5

Figure 4 – Ratio of observed to predicted (by BA08) PSA for California earthquakes
(NC=northern, SC=southern) of 5.0≤**M**<5.5, at periods 0.3 and 3s. Data are shown
for both the SMM and NGA datasets. Heavy solid boxes show mean ratios (and
standard deviation) in distance bins for SMM; means are also shown for the NGA
dataset. Heavy line shows function chosen to represent the mean trend (**M**5.25).

Figure 5 – Ratio of observed to predicted (by BA08) PSA for California earthquakes (NC=northern, SC=southern) of 5.5≤$\mathbf{M}$<6.0, at periods 0.3 and 3s. All data in this magnitude range are from the NGA dataset. Boxes show the mean ratios (and standard deviation) in distance bins (NGA), while heavy line shows function chosen to represent the mean trend($\mathbf{M}$5.75).
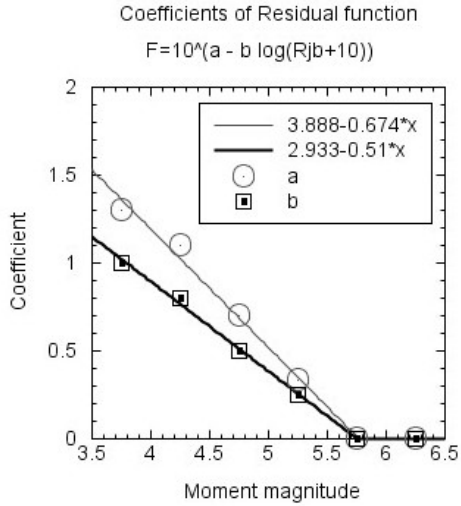
Figure 6 – Coefficients of the function, $\log(F) = a - b \log(R_{jb}+10))$, that models the residual trends, as a function of magnitude. Note that $\log(F)=0$ for **M**>5.75.
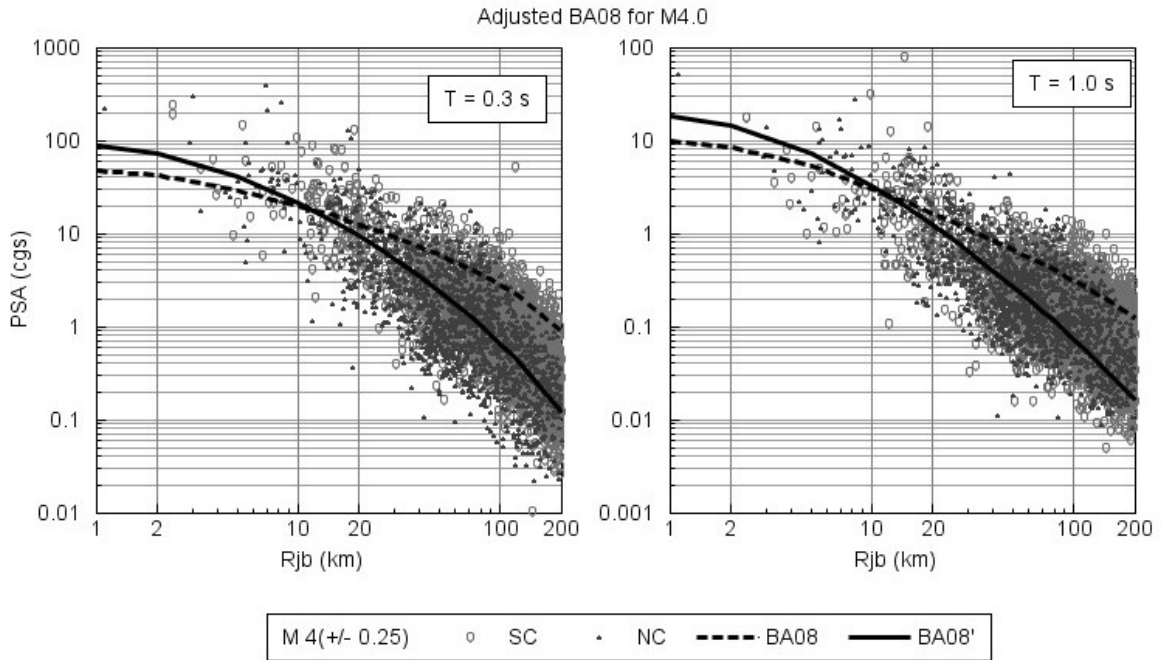
Figure 7 – Comparison of predicted PSA for adjusted BA08 equations (BA08') for **M**=4.0 (solid line) with PSA for original BA08 equation (dashed line), and with data in the magnitude range 3.75≤**M**<4.25, from northern (NC) and southern (SC) California.
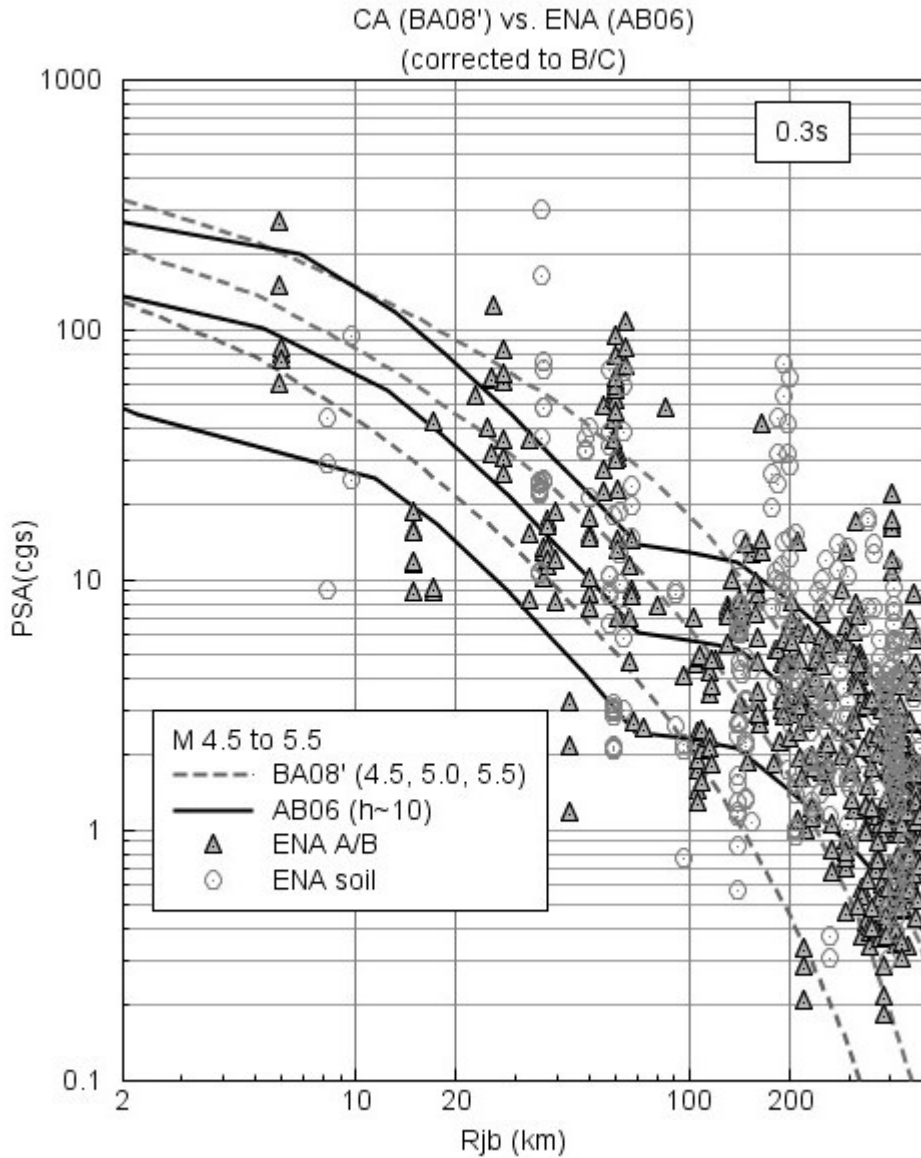
Figure 8 – Comparison of AB06 (focal depth near 10 km) and BA08' equations for
M=4.5, 5.0 and5.5, for B/C conditions, to ENA data of 4.5≤M≤5.5, for PSA at 0.3s.
Both rock and soil data have been corrected to B/C values using soil amplification
factors, but no corrections to the data for magnitude scaling have been made.
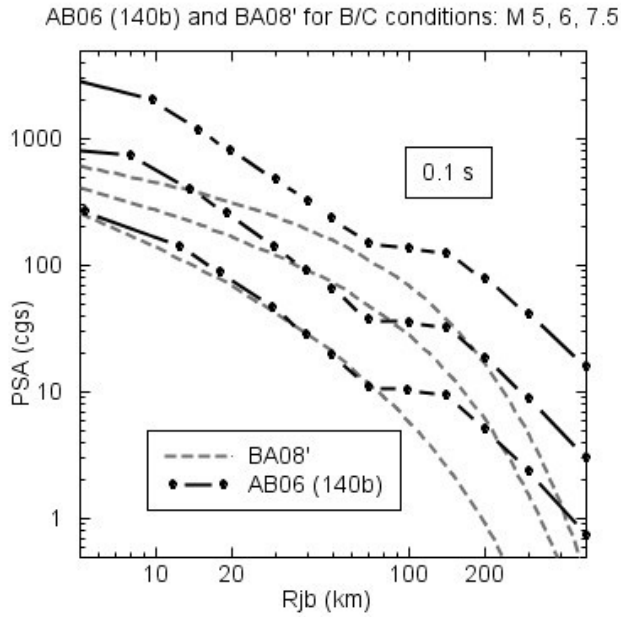
Figure 9 – Short-period magnitude scaling of original AB06 GMPEs (with 140 bar stress) compared to that of adjusted BA08', for **M**=5., 6., and 7.5.
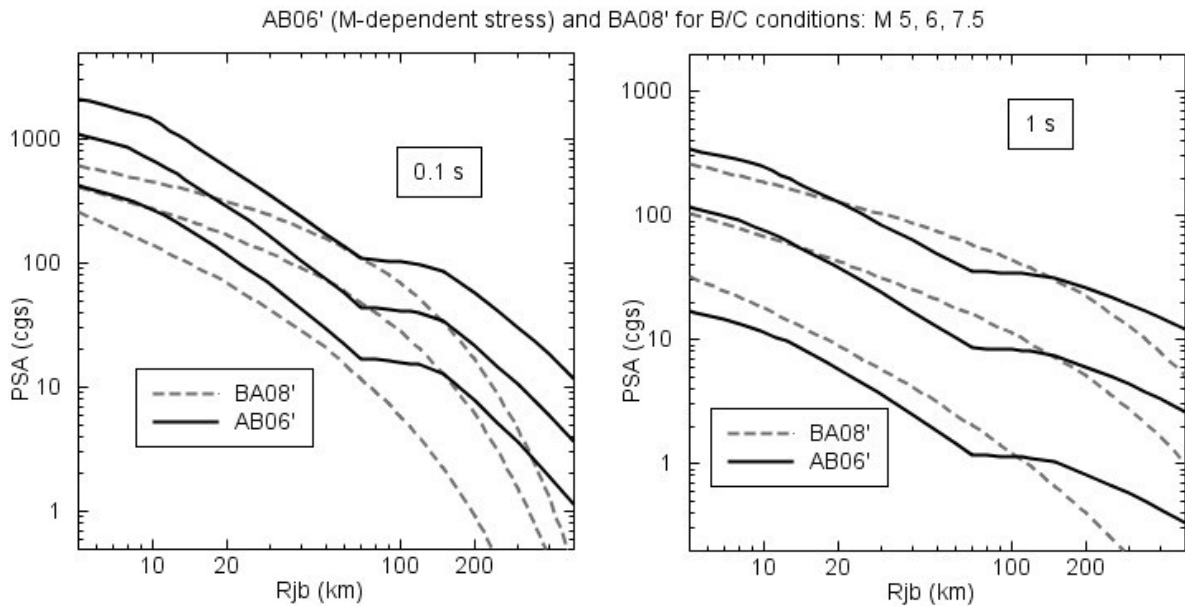
Figure 10 – Comparison of AB06' equations (implementing magnitude-dependent stress drop) with BA08' equations, for **M**5, 6 and 7.5, at periods of 0.1 and 1.0s.
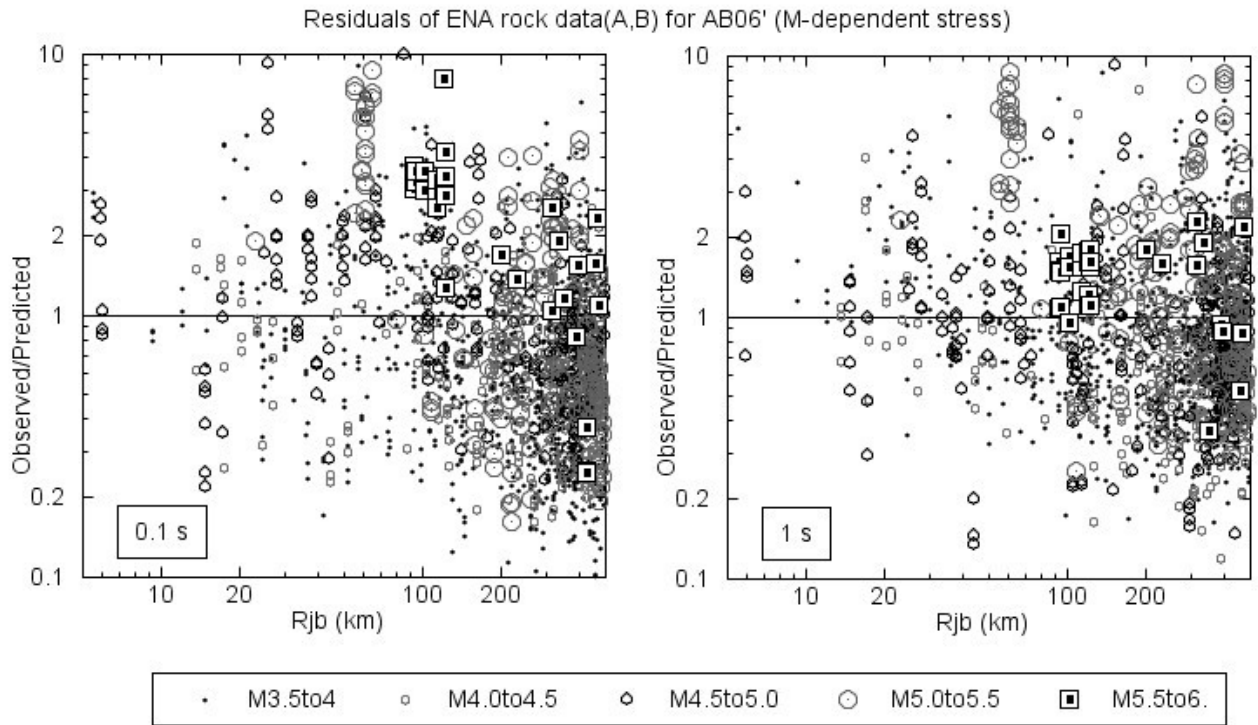
Figure 11 –Ratio of Observed/Predicted ENA rock data with respect to AB06'
predictions (magnitude-dependent stress), for periods of 0.1s and 1 s; data are
plotted for **M**≥3.5. Data in the **M**5.5 to 6.0 range are all from the 1988 Saguenay
earthquake.
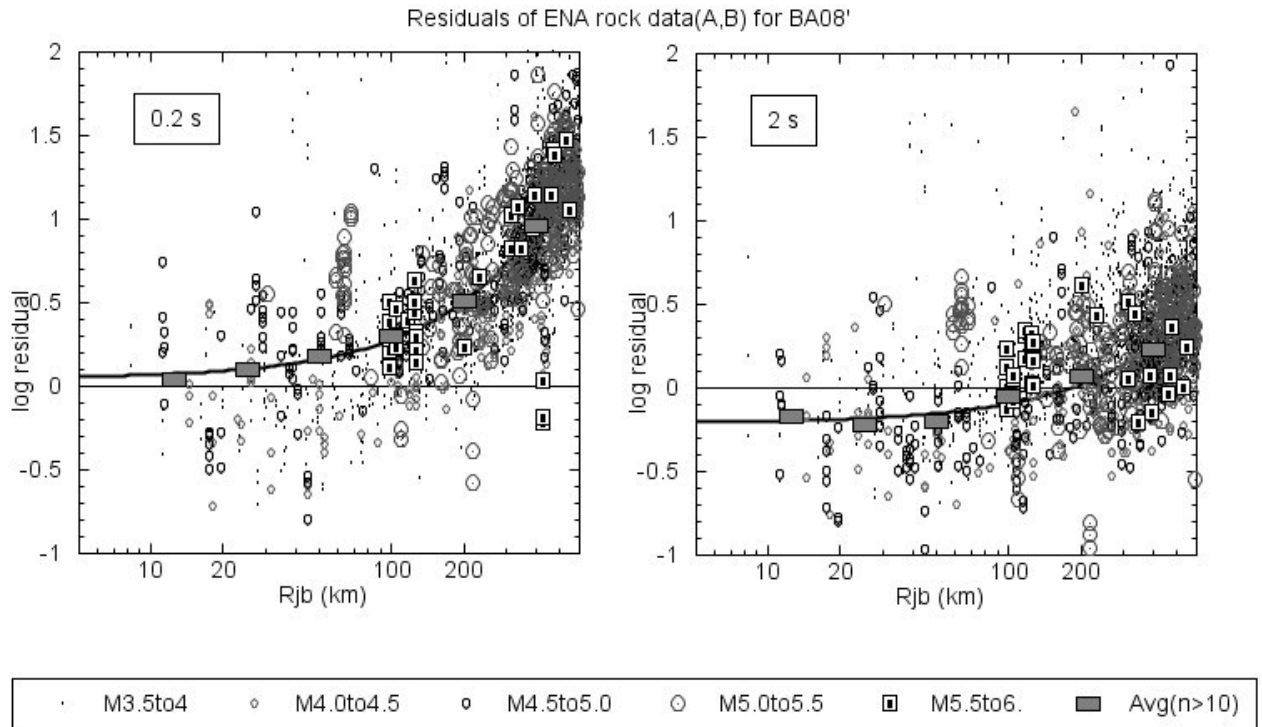
Figure 12 – Ratio of Observed/Predicted ENA rock data (log units), adjusted to B/C site conditions, versus BA08' GMPE, for 0.2s and 2.0s. Heavy filled symbols show mean residuals (log10 units) for **M**4.0 to 6.0 data in distance bins 0.3log units (factor of two) in width. Heavy solid line shows fit to log (Observed/Predicted) = $c + d\ R_{jb}$. Data in the **M**5.5 to 6.0 range are all from the 1988 Saguenay earthquake.
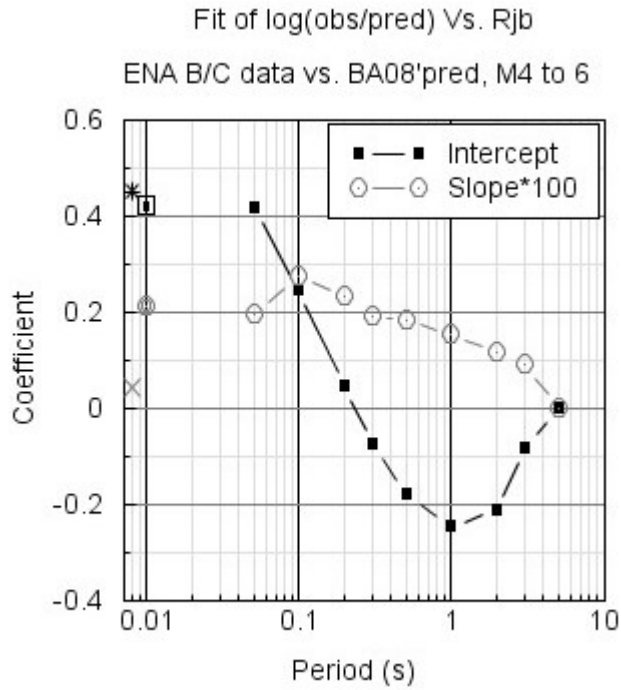
Figure 13 - Coefficients of the A08' Referenced Empirical GMPE factor: $\log F = c + d$ R_{jb} (c is the intercept and d is the slope). Note that the slope has been multiplied by a factor of 100 for plotting purposes only; actual coefficient values given in Table 4.
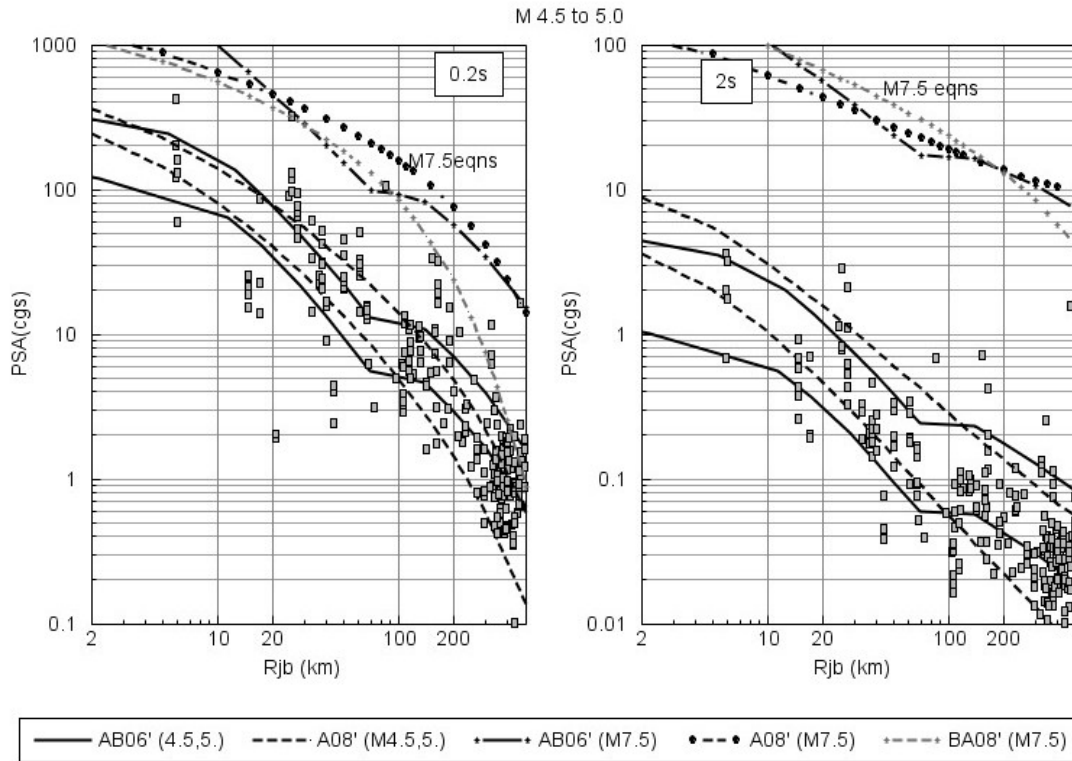
Figure 14 – Comparison of ENA ground-motion data (A/B sites) for events of 4.5≤**M**<5
with AB10 Referenced Empirical GMPE and AB06'(M-dependent stress) GMPE for
0.2s and 2.0s. Equations are shown for **M**4.5 and **M**5.0. For reference, the two ENA
GMPEs are also compared with BA08, for an event of **M**7.5.

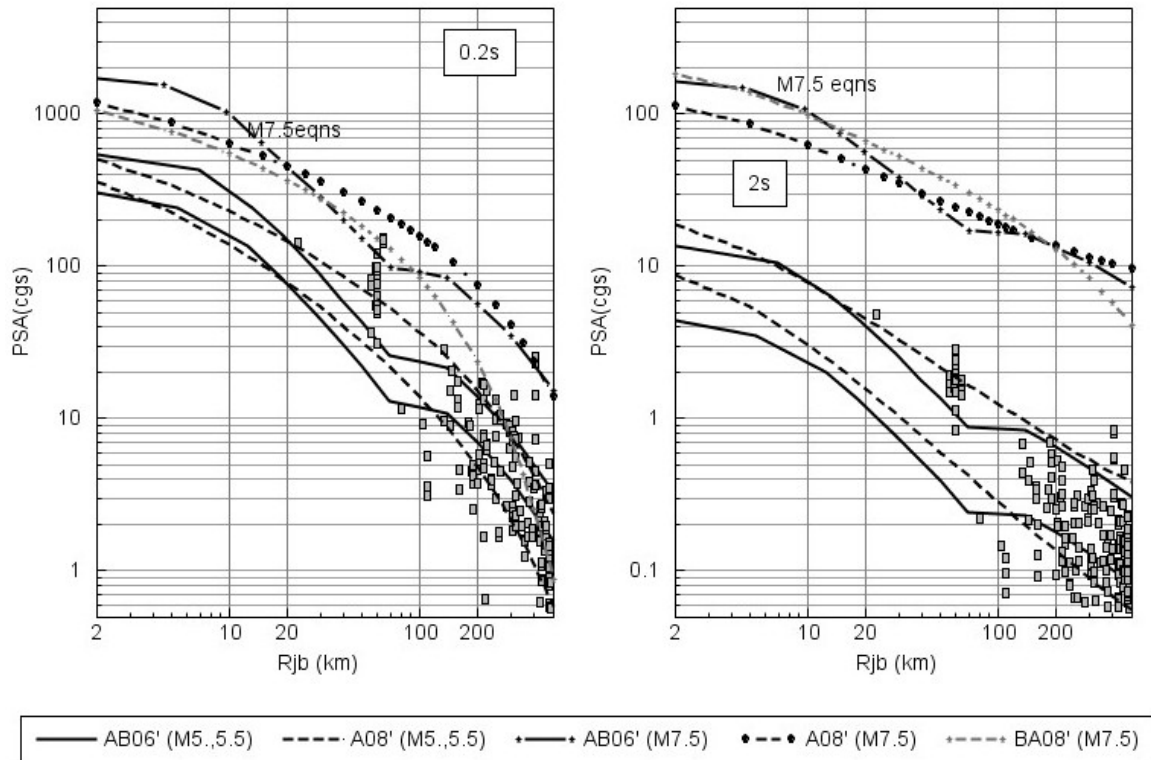ENA rock data compared to A08'(Ref.Emp.) and AB06'(M-dependent stress): for B/C

M 5.0 to 5.5

Figure 15 – Comparison of ENA ground-motion data (A/B sites) for events of

5.0≤**M**<5.5 with AB10 Referenced Empirical GMPE and AB06' (M-dependent

stress) GMPE for 0.2s and 2.0s. Equations are shown for **M**5.0 and **M**5.5. For

reference, the two ENA GMPEs are also compared with BA08, for an event of **M**7.5